Introduction of a wavelet transform based on 2D matched filter in a Markov Random Field for fine structure extraction: Application on road crack detection

Sylvie Chambon[a] and Peggy Subirats[b] and Jean Dumoulin[a]

[a]LCPC, Laboratoire Central des Ponts et Chaussées, Bouguenais, France
[b]CETE, Centre d'Études Techniques de l'Équipement, ERA 34, Rouen, France

ABSTRACT

In the context of fine structure extraction, lots of methods have been introduced, and, particularly in pavement crack detection. We can distinguish approaches based on a threshold, employing mathematical morphology tools or neuron networks and, more recently, techniques with transformations, like wavelet decomposition. The goal of this paper is to introduce a 2D matched filter in order to define an adapted mother wavelet and, then, to use the result of this multi-scale detection into a Markov Random Field (MRF) process to segment fine structures of the image. Four major contributions are introduced. First, the crack signal is replaced by a more real one based on a Gaussian function which best represents the crack. Second, in order to be more realistic, *i.e.* to have a good representation of the crack signal, we use a 2D definition of the matched filter based on a 2D texture auto-correlation and a 2D crack signal. The third and fourth improvements concern the Markov network designed in order to allow cracks to be a set of connected segments with different size and position. For this part, the number of configurations of sites and potential functions of the MRF model are completed.

Keywords: Segmentation, wavelet transform, 2D matched filter, Markov Random Field (MRF), road crack

1. INTRODUCTION

Detecting fine structures is very helpful in a lot of domains: to extract ceramic damages[1], to find cracks in underground pipes[2], to detect road network in satellite images[3], to follow vessels in medical images[4]. Since 1990, a lot of algorithms have been proposed in the domain of crack detection on road pavement surface. In fact, every country needs to evaluate, periodically, the quality of the roads and most of this work is done manually which is expensive, non reproducible, dangerous and not very efficient. In consequence, a lot of efforts have been made in the field of research on automatic procedures or semi-automatic ones for detecting deterioration on the road and, in particular detecting cracks. In 2003, the report of Schmidt[5] gives a good summary of the developed technologies in this field.

For crack detection on road pavement surface, three important elements have to be taken into account: acquisition of images, storage of data (acquiring images of a piece of national road corresponds to a huge amount of data) and image processing in order to extract the areas of deterioration. In this paper, we only describe the last part: the image processing. An illustration of the kind of difficulties of crack detection in road images is given in Figure 1. In most of the existing papers and in this paper, a crack is defined as follow:

> A crack is a set of pixels that are darker than the background. Moreover, a crack can be defined as a set of connected small segments of different orientations.

In this paper, we can distinguish approaches based on a threshold, methods employing mathematical morphology[6] or neuron networks[7] and, more recently, techniques that use an initial transformation of the image, like, for example, wavelet transform[8]. Few methods are based on wavelet decomposition for detection of road cracks. However, it allows independence from scale, size and orientation of the fine structures detected. Consequently, this work concerns the introduction of a 2D matched filter to define the mother wavelet for extracting fine

E-mail: sylvie.chambon@lcpc.fr

structures applied in the field of road crack detection. After an initial selection, some refinements can be done, like morphological operations, computation of connected regions or segmentation. Some methods, which are strongly local, are based on segmentation with Markov Random Field (MRF). In this work we suppose that cracks are connected segments, consequently, it is very advantageous to consider a local method like MRF-based one. This is why, we introduce the adapted filter decomposition into a MRF-based segmentation.

First, we present a summary of crack detect in the literature. Then, in the second section, we introduce how wavelet decomposition can be used in the context of fine structure extraction. In the third section, we explain how this extraction can be refined by segmenting the image with a MRF-based segmentation. Our experimental protocol is then detailed and conclusions and perspectives are drawn.

2. FINE STRUCTURES DETECTION

2.1 Essential steps

Numerous methods have been introduced and, in order to describe all these methods, in a generic way, we have distinguished these different steps that can be executed in order to detect fine structures:

1. *Pre-processing* to eliminate noises or enhance the contrast;
2. *Binarisation*, to extract pixels that belong to a crack;
3. *Segmentation*, to refine the first extraction, for example, for estimating the whole shape of the crack;
4. *Post-processing*, to correct errors of segmentation;
5. *Classification*, to characterize the whole crack and determine to which category it belongs.

Steps 1 and 4 are not essential but strongly recommended in order to improve the results. In a lot of proposed methods, steps 2 and 3 are not distinguished. In this paper, the wavelet-based analysis corresponds to step 2 whereas the MRF-based segmentation corresponds to step 3. In most of methods, the classification step is trivial because all the characteristics of the classes are known and, consequently, easy to separate. This is why, there is not a lot of publications on this aspect. We briefly describe all the existing work following these steps.

Pre-processing is of two interests: to improve the quality of the image, for simplifying detection[1,2,7,9], and to estimate attributes used for detection, like a Laplacian[10].

Binarisation methods are based on: thresholding[7], morphological tools[1,2,6], neuron networks[11], filtering[12] and wavelet decomposition[8]. Thresholding methods are the most frequent but also the oldest ones. The algorithms are based on: histogram analysis[13], adaptive thresholding[1], Gaussian model[14] or relaxation[15]. These methods are quite simple but not efficient and results contain noises. This is why a lot of methods based on thresholding are refined with tools of mathematical morphology[1,2,6]. Unfortunately, all these methods are very dependent of the parameters. Neuron networks have been widely employed but the most important drawbacks is the necessity of a learning step. Consequently, more recent methods, considered as the most efficients, are based on filtering[12] and, in particular wavelet decomposition[8,16].

Segmentation methods are a simple refinement of the detection by estimating connected components[9], or closing contours[13], or by analyzing the shape[2]. Other algorithms are based on merging the results of several detections, as the work of Tanaka *et al.*[6]. And, finally, more recent methods are based on neuron network[7], probabilistic segmentation[14] and Markov network[8,12].

Both goals of *post-processing* are corrections of errors (induced by the binarisation or the segmentation)[7] or extraction of attributes that are needed for establishing a classification of cracks[9].

Some *classification* methods consider only two classes: transverse and longitudinal cracks[13] or with and without cracks[17]. However some more sophisticated ones also include oblique and alligator crack[14]. All these classes are illustrated in Figure 1. If the criteria for characterizing classes of cracks are known, after extracting the attributes, it is easy to classify[9,13]. If the criteria are not known priory, they can be estimated by learning and the classification is done by a neuron network[7,10,12,18]. Some methods are based on hierarchical classification, *i.e.* classification is done per bloc and then merge to give a result for the whole image[14]. There is not a lot of literature about this aspect and, in this work, we will not discuss about this step.

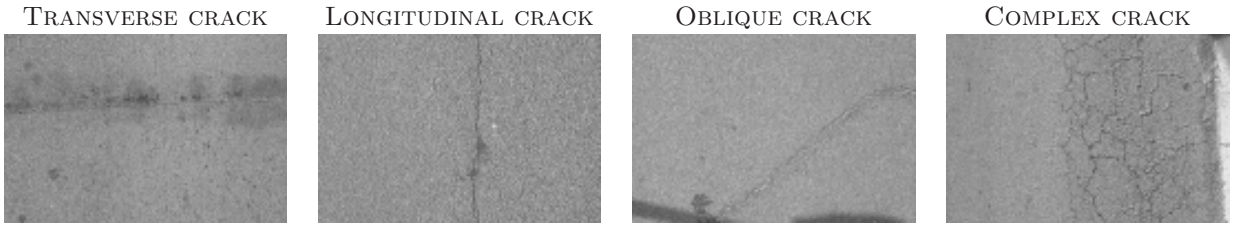

Figure 1. Examples of road surfaces with damages – These examples illustrate the difficulty of the problem: the lights are different, the road textures are not the same, some shadows or object can be present on the road.

2.2 Families of methods

Thresholding[9,13,14] (1992–1999)	Morphology[6] (1998)	Neuron network[7,10,11,18] (1991–2006)	Transform[8,12,16,17] (1990–2006)

Table 1. Families of methods for detecting cracks – There is all the references about this subject cited in this paper and in brackets, we precise the years of the cited publications.

Consequently to this state of the art, we propose to enumerate the four following families of methods: thresholding methods (with a lot of variants for the selection of the threshold), methods based on morphological tools (it corresponds to algorithms that combine thresholding and refinement with mathematical morphology), neuron networks (these methods need a step of learning), methods using transformations (these methods are based on different kind of filtering, like wavelet decomposition).

3. ALGORITHM OF THE WAVELET AND MRF-BASED METHOD

Input
Road image in gray levels

Init
- Select the number of scales
- Select the number of orientations

Steps

1. For each scale Do Estimate the adapted filter
2. For each orientation Do Apply the adapted filter
3. Aggregate the result through the orientations
4. For each scale Do
   (a) Estimate the initial sites of the Markov Random Field
   (b) While Stop condition is not true Do Update the sites

Figure 2. Algorithm of the crack detection process – While the three first steps of this algorithm concern the detection of pixels that belong to a crack, the step 4 refines this first result by using a MRF-based segmentation. Steps 1, 4a and 4b are respectively described in sections 4, 5.2 and 5.3. Details about steps 3 are given for the experimentation, section 6.

The Figure 2 presents the work-flow of the method. First of all, the initial parameters have to be fixed. As wavelet transform is used, the number of scales has to be determined. This choice depends on the minimal size of cracks that the application needs to detect and the size each pixel represents on the ground, the *resolution*. The

number of orientations depends on the type of cracks that will be detected (transverse, longitudinal, oblique). All the details about these choices are given in section 6.1. Second, the adapted filter has to be estimated and this step will be particularly detailed in section 4. Third, the detection is refined by a segmentation and the section 5 describes the novelties of the method about the definition and the updating of the MRF sites.

4. WAVELET-BASED DETECTION

In a previous work[8] a 2D matched filter has been proposed in order to extract fine structures. This method and the two improvements proposed in this paper are presented.

4.1 Wavelet definition

The function $\psi \in \mathcal{L}^2(\mathbb{R}^2)$ is a wavelet if:

$$\int_{\mathbb{R}^2} \frac{|\Psi(\mathbf{x})|^2}{\|\mathbf{x}\|^2} d\mathbf{x} < \infty, \text{with } \mathbf{x} = (i,j) \text{ and where } \Psi \text{ is the Fourier transform of } \psi. \tag{1}$$

It implies that $\int_{\mathbb{R}^2} \psi(\mathbf{x}) d\mathbf{x} = 0$. The wavelet family is built for each scale w and for each translation $\mathbf{u}$:

$$\psi_{w,\hat{u},\theta}(\mathbf{x}) = \frac{1}{\sqrt{w}} \left[R^{-\theta} \psi \left(\frac{\mathbf{x} - \mathbf{u}}{w} \right) \right], \tag{2}$$

where $\psi \in \mathbb{R}^2$ and $R^{-\theta}$ is a rotation of angle θ defined by : $\begin{pmatrix} \cos\theta & \sin\theta \\ -\sin\theta & \cos\theta \end{pmatrix}$.

One of the main difficulties to apply a wavelet decomposition concerns the choice of the mother wavelet ψ. Numerous functions are used in the literature: Haar wavelet, Gaussian derivatives, Mexican hat filter, Morlet wavelet. It is very hard to determine which one best fits an application. In the case of crack detection, two elements are present: the crack (if there is a crack) and the background (the road surface can be viewed as a repetitive texture) and it leads to the investigation on adapted filter to determine the mother wavelet.

4.2 Adapted filter

If s is a discrete and deterministic signal with values stored in the vector $\mathbf{s} = \begin{pmatrix} s_1 & \dots & s_N \end{pmatrix}$, N the number of samples, and $\mathbf{z} = \begin{pmatrix} z_1 & \dots & z_N \end{pmatrix}$, is a noisy observation of s and we suppose that it is an additive noise:

$$\mathbf{z} = \mathbf{s} + \mathbf{b}. \tag{3}$$

The main hypothesis is that this second-order noise is centered and stationary, with auto-correlation function $\boldsymbol{\phi}_{bb}$ of terms $\phi_{bb_{(i,j)}} = \phi_{bb_{|i-j|}}$, independent form the signal s. The adapted filter $\mathbf{h}$ of signal $\mathbf{s}$ is defined by:

$$\mathbf{h} = \boldsymbol{\phi}_{bb}^{-1} \mathbf{s}. \tag{4}$$

The goal of the crack detection is to recognize a signal, *i.e.* the shape is known up to a factor, mixed with a noise whose its characteristics are known. Consequently, using adapted filter is well adapted to our problem: extracting singularities in coefficients estimated by a wavelet transform.

4.3 Modeling of the crack signal

The crack signal depends on the definition of the crack. In this paper, like most of the papers on this domain, crack pixels corresponds to black pixel surrounded by background pixels (road pixels). This is why, in the modeling proposed in[8], a crack is a piecewise constant function:

$$f(x) = \begin{cases} -a & \text{If } x \in [-\frac{T}{2}, \frac{T}{2}] \\ 0 & \text{Elsewhere,} \end{cases} \text{ where the factor } a \text{ and the threshold } T \text{ have to be determined.} \tag{5}$$

This modeling does not correspond to a realistic representation of the crack. Because of sub-sampling, lights, orientation of the camera, the signal is more like a Gaussian function with zero mean:

$$f(x) = -a\ e^{-\frac{1}{2}\left(\frac{x}{\sigma}\right)^2}, \tag{6}$$

where a is the size of the crack and depends on σ, the deviation of the Gaussian law, *i.e.* $a = \frac{1}{\sigma\sqrt{(2\pi)}}$. Consequently, the term σ allows to fix the width of the crack (like threshold T in equation (5)).

4.4 Computation of the 2D adapted filter

As it is difficult, *i.e.* time and memory consuming, to evaluate auto-correlation texture on the whole image, in the previous work this method has been generalized to two dimensions by following these steps[8]:

1. Estimation of the 1D adapted filter $\mathbf{h}$;
2. Estimation of a 1D smooth filter $\mathbf{l}$ (Gaussian filter);
3. Computation of the 2D adapted filter $\mathbf{A}$: $\mathbf{A} = \mathbf{h} \otimes \mathbf{l}$ where $\otimes$ is the Kronecker product.

Here, we propose a new definition that is also more convenient for defining the filter in 2D:

1. Estimation of the 2D adapted filter $\mathbf{H}$;
2. Estimation of a 2D smooth filter $\mathbf{L}$ (Gaussian filter);
3. Computation of the 2D adapted filter $\mathbf{A}$: $\mathbf{A} = \mathbf{H} \times \mathbf{L}$ where $\times$ is the Hadamard product.

For the step 1, the auto-correlation function has to be estimated in 2D (we need to subsample the image in order to have reasonable execution time and less memory used) and the crack has to be modeled in 2D, *i.e.* $\mathbf{s}$ becomes $\mathbf{S} = [\ldots \mathbf{g} \ldots]^T$ where $\mathbf{g}$ contains the values of the Gaussian function, cf. formula (6). The matrix $\mathbf{S}$ has the same number of lines that $\mathbf{H}$.

5. MARKOV RANDOM FIELD

The goal of this part is to extract shapes, *i.e.* cracks, using the detection maps estimated at the first stage of the algorithm, it corresponds to steps 4a and 4b of the Figure 2. The MRF principle is introduced before the presentation of the improvements about the initialization of sites and the updating of the Markov Random Field.

5.1 Principle

The image is considered as a finite set of *sites* denoted $\mathcal{S} = \{s_1, \ldots, s_N\}$. For each site, the *neighborhood* is defined by: $\mathcal{V}_s = \left\{ s^{'} | s \notin \mathcal{V}_{s'} \ \&\ s^{'} \in \mathcal{V}_s \Rightarrow s \in \mathcal{V}_{s'} \right\}$. A *clique* c is defined as a subset of sites in $\mathcal{S}$ whose every pair of distinct sites are neighbors.

The random fields considered are:

1. The observation field $Y = \{y_s\}$ with $s \in \mathcal{S}$. Here, y_s is the mean of wavelet coefficients on the site.
2. The descriptor field $L = \{l_s\}$ with $s \in \mathcal{S}$. For this work, if there is a crack $l_s = 1$ elsewhere $l_s = 0$.

MRF model is well suited to take into account spatial dependencies between the variables. Each iteration, a global cost, or a sum of *potentials*, that depends on the values of the sites and the links between neighborhoods is updated. The next section introduces how sites are Modeling and then, how potential functions are defined and updated.

5.2 Modeling and initialization of sites

In step 4a of the algorithm presented in Figure 2, in[8], the sites are of size 3×3, consequently, a regular grid is considered on the image. The four configurations that are possible, are represented in Figure 3. The initialization of the sites is based on the configuration that maximizes the wavelet coefficients. More formally, if we denoted $\gamma_{2,0}$, $\gamma_{2,\frac{\pi}{4}}$, $\gamma_{2,\frac{\pi}{2}}$ and $\gamma_{2,\frac{3\pi}{4}}$, cf. in the bold rectangle in Figure 3, the four configurations, the best configuration γ_{best} is obtained with:

$$\gamma_{\text{best}} = \underset{\alpha \in \left[0..\frac{3\pi}{4}\right]}{\text{argmax}}\, m_{2,\alpha}, \tag{7}$$

where $m_{2,\alpha}$ is the mean of wavelet coefficients on the considered configuration $\gamma_{2,\alpha}$. These four configurations do not represent all the possible and realistic configurations. In fact, all these four configurations are centered, whereas, it is possible to have some non-centered configurations. Consequently, we decided to introduce a set of configurations that includes this aspect and we propose a set of sixteen configurations illustrated in Figure 3. By modifying the number of configurations, we need to adapt the initialization of sites, *i.e.* equation (7).

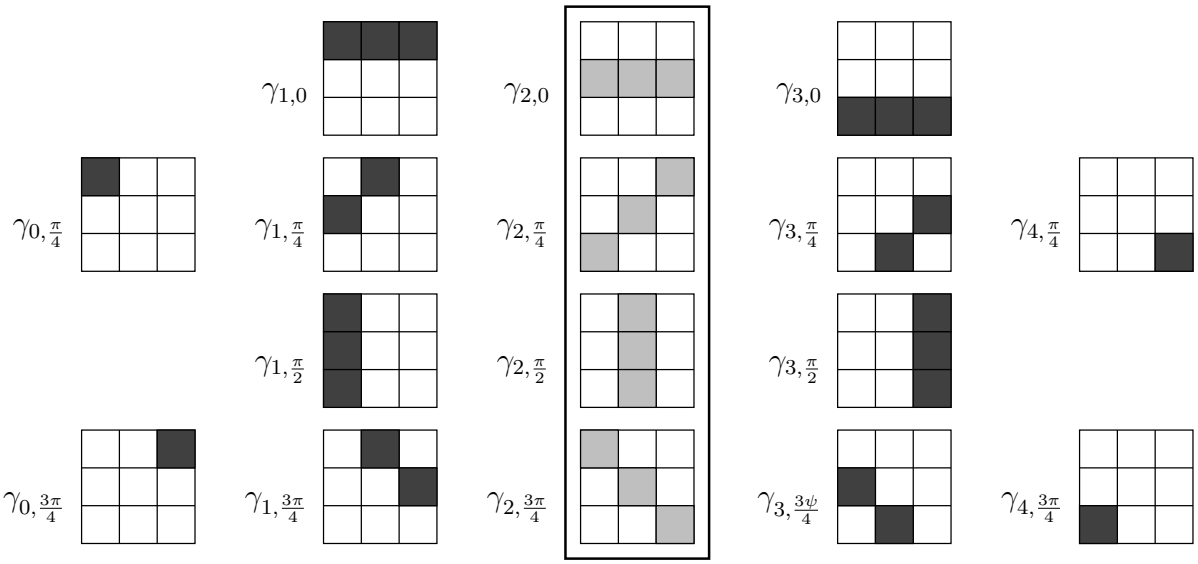

Figure 3. The sixteen configurations in order to improve the modeling of sites – The four initial configurations proposed in[8] are in the bold rectangle, the sites are represented by the clearer gray levels, and for the proposed configurations the sites are represented by the darker gray levels.

5.3 Updating of the Markov network

At each step, a global cost is updated. This global cost takes into account the site coefficients (computed from the wavelet coefficients estimated during the three first steps of the algorithm in Figure 2, cf. section 4) and the relation between each site and the sites in his neighborhood (in this paper, in the eight vicinities). More formally, the global cost is the sum of all the potentials of the sites. This potential is composed of two terms and defined by:

$$u_s(s) = \alpha_1 u_1(s) + \alpha_2 \sum_{s' \in \mathcal{V}_s} u_2(s, s'), \text{ where } \mathcal{V}_s \text{ is the neighborhood of site } s. \tag{8}$$

The choice of the values α_1 and α_2 depends on the importance of each part of the equation (8). In the section 6, our choice for these parameters and all the other parameters presented in this part is given.

The function u_1 is given by:

$$u_1(y_s, l_s = 1) = \begin{cases} e^{\xi_1 (k - y_s)^2} & \text{If } y_s \geq k \\ 1 & \text{Elsewhere} \end{cases} \text{ and } u_1(y_s, l_s = 0) = \begin{cases} e^{\xi_2 (y_s - k)^2} & \text{If } y_s < k \\ 1 & \text{Elsewhere,} \end{cases} \tag{9}$$

The parameters ξ_1, ξ_2 and k have to be fixed. The choice of k is related to the maximal number of pixels that belong to a crack (it depends on the resolution of images and hypothesis about the size and configuration of cracks). For the definition of u_2, we have to determine the number of cliques. In[8], four cliques are possible. As there is four configurations in the previous approach, there is sixteen possibilities. A 8-neighborhood is considering but the potential function proposed in the precedent work only considers the difference of orientations between two neighborhoods and not the position between the two sites of the clique, cf. Table 2.

	$\gamma_{2,0}$	$\gamma_{2,\frac{\pi}{4}}$	$\gamma_{2,\frac{\pi}{2}}$	$\gamma_{2,\frac{3\pi}{4}}$
$\gamma_{2,0}$	β_1	β_2	β_3	β_2
$\gamma_{2,\frac{\pi}{4}}$	β_2	β_1	β_2	β_3
$\gamma_{2,\frac{\pi}{2}}$	β_3	β_2	β_1	β_2
$\gamma_{2,\frac{3\pi}{4}}$	β_2	β_3	β_2	β_1

Table 2. Function u_2 – This table represents the values of the function $u_2(s^{'}, s)$ for the sites in clearest Gray level in Figure 3. In the experiments we have taken the values of the parameters proposed by the authors[8], that allow the best results: $\beta_1 = -2$, $\beta_2 = -1$ and $\beta_3 = 2$.

Some cases are not penalized with the old configuration. For example, these two unfavorable cases are not penalized: two sites with same orientation but with no connection between them, two sites with the same orientation but their position makes them parallel. This is why, with the sixteen possible configurations presented in Figure 3, the new variant takes into account differences of orientations between two sites (there is 16×16 possibilities) and position of the two sites (there is eight possibilities because of 8-connexion). Consequently, the new potential function u_2 follows these two important rules:

1. The lower the distance between two sites, the lower the potential (in this case, distance means the minimal distance between the extremities of the two segments).
2. The lower the difference of orientations between two sites, the lower the potential.

More formally, if d denotes the Euclidean distance between the two closest extremities of the sites, with $d \in [0, d_{\max}]$, with $d_{\max} = 5\sqrt{2}$ and θ_1 and θ_2, the orientations of respectively $s = \{s_i\}_{i=1..N_s}$ and $s^{'} = \{s_j^{'}\}_{j=1..N_{s'}}$ and θ_e the angle between the two sites, the u_2 function is defined by:

$$u_2(s', s) = \begin{cases} d_{\max}\text{NbC} & \text{If } \theta_1 = \theta_2 \quad \text{and} \quad \theta_1 = \theta_e \\ |\theta_e - \theta_1| - d_{\max}\text{NbC} & \text{If } \theta_1 = \theta_2 \quad \text{and} \quad \theta_1 \neq \theta_e \quad \text{and} \quad \text{NbC} \neq 0 \\ |\theta_e - \theta_1| + \min\limits_{i,j}(d(s_i, s_j^{'})) & \text{If } \theta_1 = \theta_2 \quad \text{and} \quad \theta_1 \neq \theta_e \quad \text{and} \quad \text{NbC} = 0 \\ |\Delta\theta_{e,1} - \Delta\theta_{e,2}| - d_{\max}\text{NbC} & \text{If } \theta_1 \neq \theta_2 \quad \text{and} \quad \text{NbC} \neq 0 \\ |\Delta\theta_{e,1} - \Delta\theta_{e,2}| + \min\limits_{i,j}(d(s_i, s_j^{'})) & \text{Elsewhere,} \end{cases} \tag{10}$$

where NbC indicates the number of elements of the two sites s and $s^{'}$ that are connected (in the neighborhood of each other). The term $\Delta\theta_{e,i}$ with $i \in [1, 2]$ is defined by $\mid \theta_e - \theta_i \mid$. The first case of the equation (10) is the best situation whereas the third one is the worst case. The last case is also a bad situation.

6. EXPERIMENTATION

6.1 Protocol

In the global process of crack detection presented in paragraph 2.1, we do not consider the step 1. For step 4, a Hough transform is applied. In fact, the goal of this work was to present the efficiency of the binarisation based on wavelet (step 2) and of the MRF-based segmentation (step 3) and this is why the pre-processing and post-processing are very simple. Moreover, the goal was not to present a new classification method, and step 5 has not been implemented for these tests. Consequently, for experimentation we simply used the algorithm

presented in Figure 2. The different parameters for the wavelet decomposition are the scales $\in [1, 2, 3, 4, 5]$ and the number of orientations $\in [0, \frac{\pi}{4}, \frac{\pi}{2}, \frac{3\pi}{4}]$. The mean for aggregating the results is a sum.

For the Markov network, for the potential functions, equation (8), as in[8], $\alpha_2 = 2\alpha_1$ because we want to increase the influence of the spatial dependencies which is represented by the second term. Moreover, the optimization is the well-known method of the Iterated Conditional Modes (ICM)[19]. For the equation (9) we have chosen $\xi_1 = \xi_2 = 100$ and k is fixed in order to label 5% of the pixels as crack pixels (5% represent the maximal percentage obtained with an alligator crack that covers all the image with 30 cm between each crack).

We have tested sixty-four images that represent all the kind of cracks: transverse (thirty-two), alligator or complex (composition of oblique and transverse)(twenty), longitudinal (eight) and oblique (four), cf. Figure 1. We have not tested images with no damage because the aim of the proposed method is not to propose a crack classification but a crack detection. These images are a significant sample with different kind of road textures, and it also contains difficult images (with shadows, oil stains, repaired crack, road marking, objects).

6.2 Results

In order to observe the improvement obtained for the two new parts of this work we made two kinds of experimentation: one with new adapted filter and old Markov Modeling (comparison with old adapted filter) and one with new adapted filter and new Markov Modeling (comparison with old adapted filter too).

Improvement of Binarisation – First of all, we comment the results obtained with three different versions of the algorithm for the Binarisation:

1. `Old`: the algorithm presented in[8];
2. `New_signal`: the signal is represented by a Gaussian function, cf. section 4.3;
3. `New_signal_2D`: the signal is like in `New_signal` and the auto-correlation is estimated in 2D, cf. 4.4.

For all these algorithms, the MRF segmentation is like in[8]. The results are summarized in Table 3. It illustrates how much we obtained best results with the two new variants in comparison with the old one. Visually, the results of the two new methods are quite near, but, it seems that the complete version, `New_signal_2D` obtains good results with images with difficulties: road marking, objects. However, we can notice that this method does not work well in the presence of shadows, cf. Figure 4.

Method / Type	`Old`	`New_signal`	`New_signal_2D`	Total
Transverse	2	**15**	**15**	32
Complex	1	6	**13**	20
Longitudinal	0	1	**7**	8
Oblique	1	1	**2**	4
Total	4	23	**37**	64

Table 3. Results obtained with three variants of detection based on wavelet decomposition – Each value represents the number of images where the method obtained the best binarisation. Best results are highlighted in bold letters. These results illustrate the superiority of `New_signal_2D` and the good results obtained with `New_signal`.

Improvement of segmentation – We compared the results obtained with the three versions for the binarisation, cf. the previous paragraph, and the three versions of the Markovian Modeling:

1. `Old_Markov`: the algorithm presented in[8] with new MRF, cf. section 5;
2. `New_signal_Markov`: the signal is a Gaussian function, cf. section 4.3, with new MRF, cf. section 5;
3. `New_signal_2D_Markov`: the signal is like in `New_signal` and the auto-correlation is estimated in 2D, cf. 4.4, with new MRF, cf. section 5.

For all these three last versions, compared to the versions without the new Markovian Modeling, in 60% of the cases, the results are improved, in 20%, they are unchanged and in 20%, there are a bit destroyed. Some examples are given in figures 5 and 6. The methods with new MRF give less false positives than the methods without new MRF, and, on the contrary, they give less true positives. Moreover, the new ones are more precise, *i.e.* there is only one response inside the crack and not multiple responses around the cracks.

7. CONCLUSION AND PERSPECTIVES

The proposed method is based on an extraction with wavelet decomposition and a refinement by a MRF-based segmentation. Contributions concern the Modeling of the crack signal by a Gaussian function, the 2D expression of the matched filter, the complete definition of sites in the MRF and the updating of the sites using these new configurations and that takes into account the relative position between each site and its neighborhood. The results obtained highlight the superiority of new methods, in particular the method with new adapted filter in 2D combined with the new Markovian modeling, compared to the old one: they obtain visually best results, with less false detections and more robustness to changes of lighting and occluding objects than the old method. However, the experimentation also shows that new methods are more sensitive to shadows and do not always obtain the best result.

A first improvement can be to introduce more tools in the pre-processing, for example, for removing shadows. Moreover, in order to be more complete, it is necessary to add a post-processing step in order to eliminate more false detections and to add crack pixels not detected. The second improvement can be about the modeling of the 2D matched filter and in particular for estimating the auto-correlation. In this work, the auto-correlation takes into account the crack pixels and is global. It would be interesting to consider local auto-correlation and to remove (as much as possible) crack pixels. Final step of this work is to complete the experimentation by testing dynamic images and by adding a quantitative evaluation.

REFERENCES

[1] Elbehiery, H., Hefnawy, A., and Elewa, M., "Surface Defects Detection for Ceramic Tiles Using Image Processing and Morphological Techniques," *Proceedings of World Academy of Science, Engineering and Technology (PWASET)* **5**, 158–162 (Apr. 2005).

[2] Iyer, S. and Sinha, S., "A robust approach for automatic detection and segmentation of cracks in underground pipeline images," *Image and Vision Computing* **23**, 921–933 (Sept. 2005).

[3] Geman, D. and Jedynak, B., "An Active Testing Model for Tracking Roads in Satellite Images," *IEEE Transactions on Pattern Analysis and Machine Intelligence* **18**, 1–14 (Jan. 1996).

[4] Chaudhuri, S., Chatterjee, S., Katz, N., Nelson, M., and Goldbaum, M., "Detection of blood vessels in retinal images using two-dimensional matched filters," *IEEE Transactions on Medical Imaging* **8**, 263–269 (Sept. 1989).

[5] Schmidt, B., "Automated pavement, cracking assessment equipement – State of the art," Technical report 320, World Road Association (PIARC) (Oct. 2003).

[6] Tanaka, N. and Uematsu, K., "A Crack Detection Method in Road Surface Images Using Morphology," in [*Workshop on Machine Vision Applications*], 154–157 (Nov. 1998).

[7] Kaseko, M. and Ritchie, S., "A neural network-based methodology for pavement crack detection and classification," *Transportation Research Part C: Emerging Technologies information* **1**, 275–291 (Dec. 1993).

[8] Subirats, P., Dumoulin, J., Legeay, V., and Barba, D., "Automation of pavement surface crack detection with a matched filtering to define the mother wavelet function used," in [*European Signal Processing Conference*], (Sept. 2006).

[9] Cheng, H., Chen, J., Glazier, C., and Hu, Y., "Novel approach to pavement cracking detection based on fuzzy set theory," *Journal of Computing in Civil Engineering* **13**, 270–280 (Oct. 1999).

[10] Bray, J., Verma, B., Li, X., and He, W., "A Neural Nework based Technique for automatic Classification of Road Cracks," in [*International Joint Conference on Neural Networks*], 907–912 (July 2006).

[11] Ritchie, S., Kaseko, M., and Bavarian, B., "Development of an Intelligent System for Automated Pavement Evaluation," *Journal of the Transportation Research Board* **1311**, 112–119 (1991).

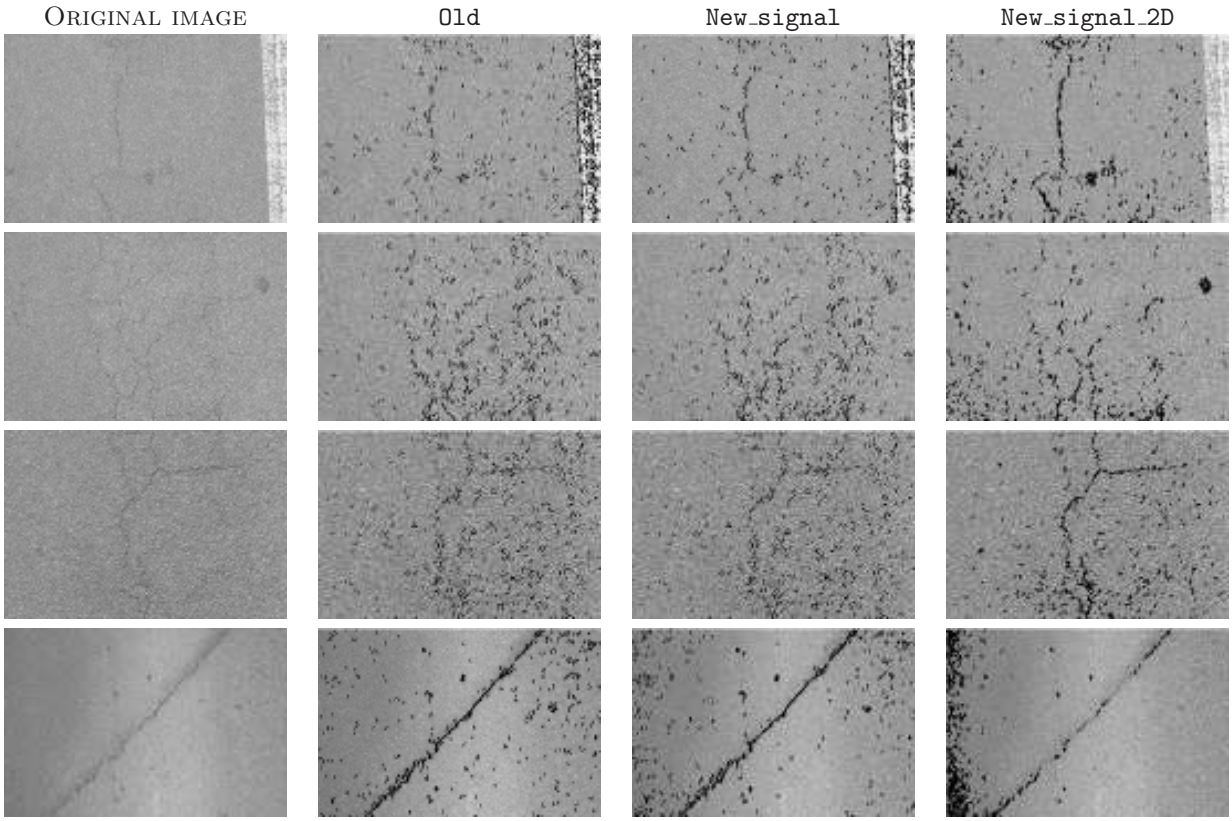

Figure 4. Segmentation results obtained for the three different variants for binarisation – The crack detection is in black (for visual aspects, this area has been dilated). The three first rows illustrate the best results obtained with `New_signal_2D` and the difficulties of the other methods, especially in the presence of road marking. In the last row, the `New_signal` gives the best result and this example shows the difficulty of `New_signal_2D` when there are shadows and also highlights the fact that `New_signal` gives less false detections than `Old`.

[12] Delagnes, P. and Barba, D., "A Markov random field for rectilinear structure extraction in pavement distress image analysis," in [*International Conference on Image Processing*], **1**, 446–449 (Oct. 1995).

[13] Acosta, J., Adolfo, L., and Mullen, R., "Low-Cost Video Image Processing System for Evaluating Pavement Surface Distress," *Journal of the Transportation Research Board* **1348**, 63–72 (1992).

[14] Koutsopoulos, H. and Downey, A., "Primitive-Based Classification of Pavement Cracking Images," *ASCE, Journal of Transportation Engineering* **119**, 402–418 (May–June 1993).

[15] Koutsopoulos, H., El Sanhouri, I., and Downey, A., "Analysis of Segmentation Algorithms for Pavement Distress Images," *ASCE, Journal of Transportation Engineering* **119**, 868–888 (Nov.–Dec. 1993).

[16] Zhou, J., Huang, P., and Chiang, F., "Wavelet-based pavement distress classification," *Journal of the Transportation Research Board* **1940**, 89–98 (2005).

[17] Fukuhara, T., Terada, K., Nagao, M., Kasahara, A., and Ichihashi, S., "Automatic pavement-distress-survey system," *ASCE, Journal of Transportation Engineering* **116**, 280–286 (May–June 1990).

[18] Chou, J., O'Neill, W., and Cheng, H., "Pavement Distress Evaluation Using Fuzzy Logic and Moment Invariants," *Journal of the Transportation Research Board* **1505**, 39–46 (1995).

[19] Besag, J., "On the statistical analysis of dirty pictures," *Journal of the Royal Statistical Society* **48**(3), 259–302 (1986).

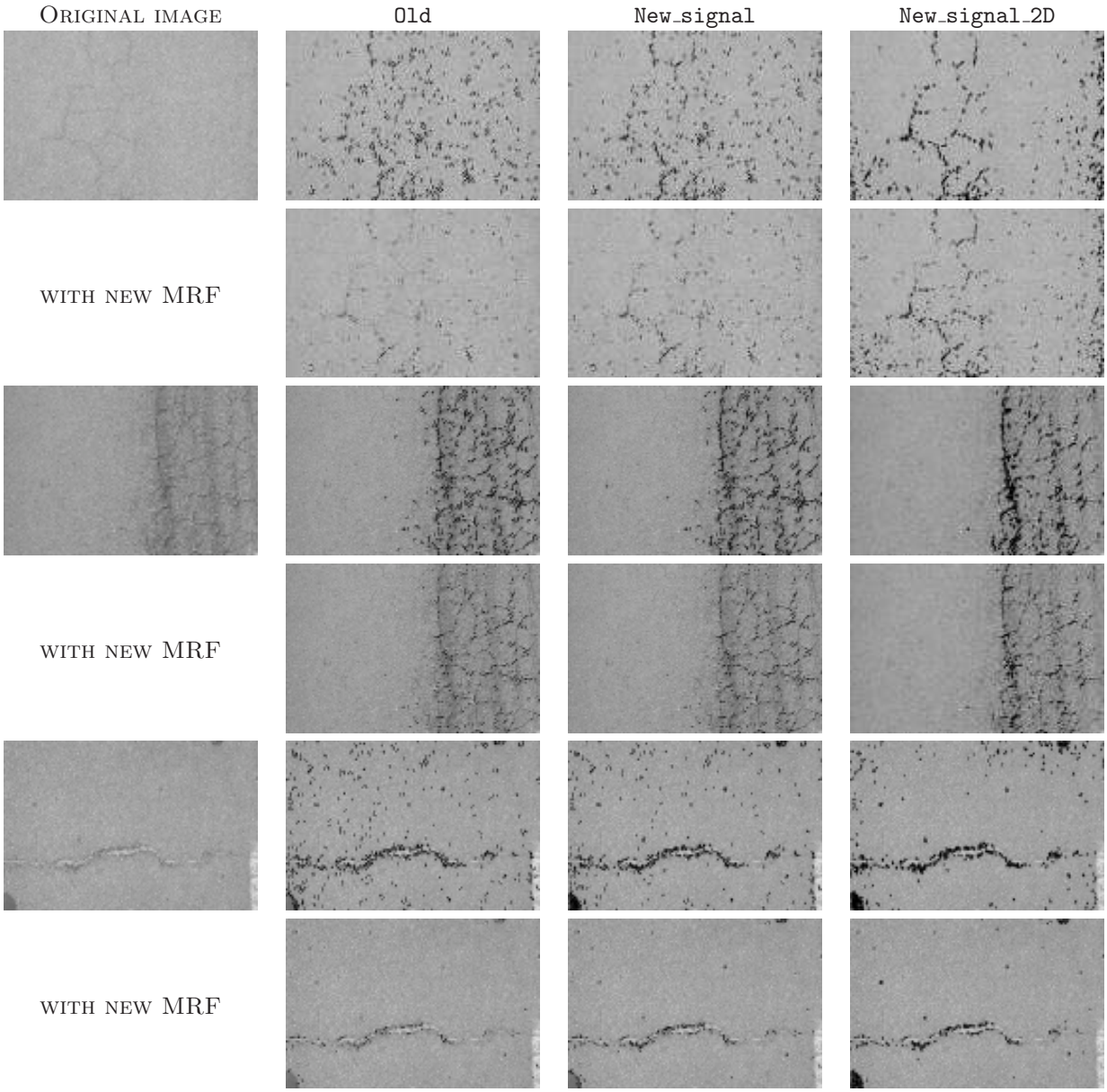

Figure 5. Segmentation results obtained for the six different variants for detection – The crack detection is in black (for visual aspects, this area has been dilated). In all the cases, the `new_signal_2D` methods give a more complete detection than the others. The main advantage of new MRF is that the segmentation is less noisy than without the new MRF (particularly in the third image).

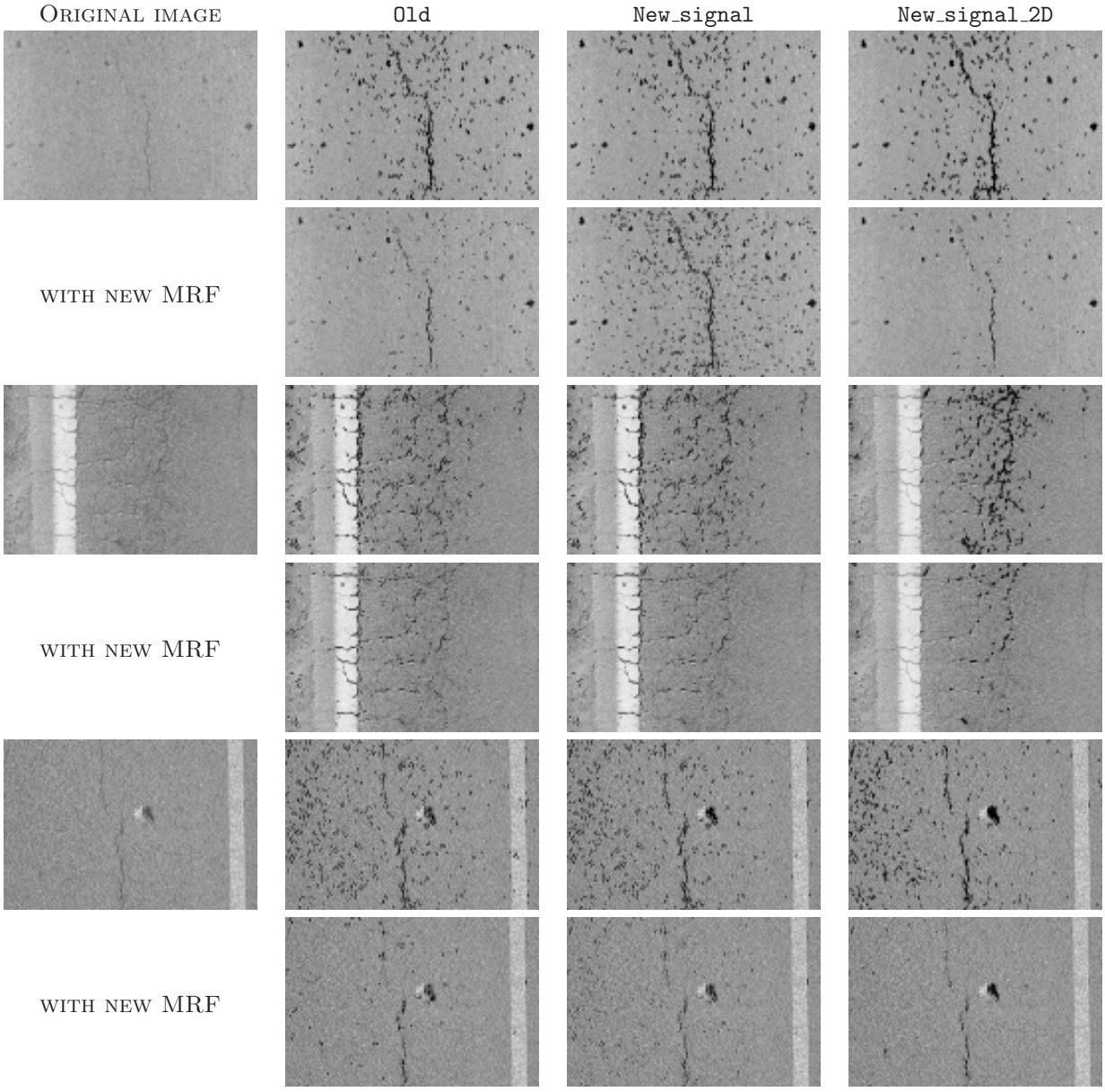

Figure 6. Segmentation results obtained for the six different variants for detection – The crack detection is in black (for visual aspects, this area has been dilated). These cases illustrate the difficulties of these new methods with MRF: sometimes only a part of the crack is detected.